



ELSEVIER

Biophysical Chemistry 89 (2001) 65–76

Biophysical  
Chemistry

www.elsevier.nl/locate/bpc

## Lens crystallins and oxidation: the special case of $\gamma$ S

Fériel Skouri-Panet<sup>a,\*</sup>, Françoise Bonneté<sup>a</sup>, Karine Prat<sup>a</sup>,  
Orval A. Bateman<sup>b</sup>, Nicolette H. Lubsen<sup>c</sup>, Annette Tardieu<sup>a</sup>

<sup>a</sup>*Laboratoire de Minéralogie-Cristallographie (LMCP), CNRS-Universités Paris VI & VII, Case 115, 4 place Jussieu, 75252 Paris cedex 05, France*

<sup>b</sup>*Department of Crystallography, Laboratory of Molecular Biology, Birbeck College, Malet Street, London WC1E 7HX, UK*

<sup>c</sup>*Department of Molecular Biology, University of Nijmegen, Toernooiveld 1, 6525 ED, Nijmegen, The Netherlands*

Received 26 June 2000; received in revised form 5 October 2000; accepted 8 October 2000

### Abstract

Among lens crystallins,  $\gamma$ -crystallins are particularly sensitive to oxidation, because of their high amount of Cys and Met residues. They have the reputation to induce, upon ageing, lens structural modifications leading to opacities. A combination of small angle X-ray scattering and chromatography was used to study the oxidation of  $\gamma$ -crystallins. At pH 7.0, all the  $\gamma$ -crystallins under study were checked to have the same structure in solution. Under gentle oxidation conditions at pH 8.0, human  $\gamma$ S (h $\gamma$ S) and bovine  $\gamma$ S (b $\gamma$ S) formed disulfide-linked dimers, whereas the other b $\gamma$ -crystallins did not. Cys20 was shown to be responsible for dimer formation since the C20S mutant only formed monomers. The h $\gamma$ S dimers were stable for weeks and did not form higher oligomers. In contrast, monomeric  $\gamma$ S-crystallins freshly prepared at pH 8.0, and submitted to more drastic oxidation by X-ray induced free radicals, were rapidly transformed into higher oligomers. So, only extensive oxidation causing partial unfolding could be detrimental to the lens and linked to cataract formation. The  $\gamma$ S-crystallins lack the temperature-induced opacification observed with the other  $\gamma$ -crystallins and known as cold cataract. The oxidation-induced associative behaviour and cold cataract are therefore demonstrated to be uncoupled. © 2001 Elsevier Science B.V. All rights reserved.

**Keywords:** Lens crystallin;  $\gamma$ S-crystallin; Oxidation; Cataract

\* Corresponding author. Tel.: +33-1-44-27-72-05; fax: +33-1-44-27-37-85.

E-mail address: skouri@lmcp.jussieu.fr (F. Skouri-Panet).

## 1. Introduction

Human lens crystallins need to keep their native structure and interactions to maintain lens transparency [1]. These proteins are exceptionally stable, since they are synthesised to last as long as human life. The major age related modifications found in the soluble crystallin fraction seem to be deamidations and disulfide bonds [2,3]. Yet, oxidation of lens crystallins has often been found associated with human cataract (see review in Spector [4]). Oxidation could contribute to the pathological events leading to cataract by promoting aggregation.

Because of their high level of thiol groups,  $\gamma$ -crystallins are usually considered likely candidates for oxidation induced oligomerisation.  $\gamma$ -crystallin oxidation has been studied through a variety of *in vitro* systems including for instance ageing at room temperature [5], vitamin C-induced oxidation [6], or  $H_2O_2$ -induced cataract on calf lenses in culture [7]. All these studies confirmed the sensitivity of  $\gamma$ -crystallins to oxidation with, possibly, a special sensitivity of  $\gamma$ S, within the  $\gamma$ -crystallin family.

Interestingly, a point mutation in the human  $\gamma$ D-crystallin ( $h\gamma$ D) gene, R14C, recently shown to be associated with an hereditary cataract [8], was demonstrated to promote *in vitro* the formation of disulfide-linked oligomers [9].

$\gamma$ S belongs to the  $\beta/\gamma$  superfamily, where the polypeptide chain consists of two domains connected by a linker peptide. Each domain comprises two Greek key motifs forming a sandwich of two four-stranded, antiparallel  $\beta$ -sheets. The domains are always found to be associated pairwise, by intermolecular contacts in oligomeric  $\gamma$ -crystallins or intramolecular associations in monomeric  $\gamma$ -crystallins. Sequence comparison shows that  $\gamma$ S is more closely related to the monomeric  $\gamma$ -crystallins (53% identity) than to the oligomeric  $\beta$ -crystallins (35%). Compared to the other  $\gamma$ -crystallins,  $\gamma$ S has a four amino-acid N-terminal extension, lacks two C-terminal amino acids and the linker peptide has an additional amino acid (Table 1). Functionally  $\gamma$ S also appears different from the other  $\gamma$ -crystallins since it is essentially expressed in the post-natal period

and is therefore preferentially located in the lens cortex (peripheral part of the lens) [10,11].

From a structural standpoint, only a few studies have been devoted to  $b\gamma$ S. Sedimentation equilibrium has shown that it was monomeric in solution at physiological pH [12]. In addition, the  $b\gamma$ S C-terminal domain has been crystallised and the three-dimensional structure was found to be similar to that of the other  $\gamma$ -crystallins [13]. Therefore, the  $\gamma$ S-crystallin three-dimensional structure has been modelled [12] on the basis of  $b\gamma$ B [14] and  $b\beta$ B2 structure [15]. Only recently, the thermodynamic characterisation of equilibrium unfolding transitions, at varying pH, of recombinant  $h\gamma$ S and  $b\gamma$ S and their isolated N- and C-terminal domains has been published [16]. Compared to  $\gamma$ B,  $\gamma$ S was found less stable.

All these results prompted us to study  $\gamma$ S-crystallin structure, interactions and oxidative behaviour in solution. We have used for our studies recombinant  $h\gamma$ S, a C20S  $h\gamma$ S mutant, and native  $b\gamma$ S. When necessary,  $b\gamma$ B and  $b\gamma$ D were used for the sake of comparison.

## 2. Materials and methods

### 2.1. Expression of $h\gamma$ S

The construction of the expression plasmid for the  $h\gamma$ S has been previously described [16]. In short, the coding sequence was amplified from a human lens cDNA library and cloned NdeI/BamHI in the pET3a vector. The expression construct was introduced into the BL21(DE3) pLysS bacterial strain. The LB medium (400 ml) containing ampicillin ( $100 \mu\text{g ml}^{-1}$ ) and chloramphenicol ( $34 \mu\text{g ml}^{-1}$ ) was inoculated with 1 ml of an overnight culture. Cells were grown until an  $OD_{600 \text{ nm}}$  between 0.3 and 0.6 was reached. Protein expression was induced by addition of isopropyl- $\beta$ -D-thiogalactoside (IPTG) to a final concentration of 5 mM at  $37^\circ\text{C}$  for 4 h under vigorous shaking. The cells were harvested by centrifugation at  $6000 \text{ rev. min}^{-1}$  for 10 min at  $4^\circ\text{C}$  and resuspended in 20 ml buffer: 50 mM Tris-HCl (pH 7.0), 100 mM glucose, 10 mM EDTA, 1.5 mM phenylmethylsulfonyl fluoride

Table 1

N-arm	
Bovine $\gamma$ B	----
Bovine $\gamma$ D	----
Human $\gamma$ S	SKTG
Bovine $\gamma$ S	SKTG
N-terminal domain	
	1   20   40   60   80
Bovine $\gamma$ B	GKITFYEDRGFGHGCYECSSDCPNLQPFSCNSIRVDSG <b>C</b> WMLYERPNYQGHQYFLRRGDYDPDYQQMMGFNDSIRSCRLIP
Bovine $\gamma$ D	GKITFYEDRGFGGRHYECSSDHSNLQPLGRCSNRVDSG <b>C</b> WMIYEQPNYLGPQYFLRRGDYDPDYQQMMGLNDSIRSCRLIP
Human $\gamma$ S	TKITFYEDKNFQGRYD <b>CD</b> CADFTLSRCNSIKVEGWTWAYERPFPAGYMYILLPQGEYPEYQRMWGLNDRLS <b>C</b> RAVH
Bovine $\gamma$ S	TKITFFEDKNFQGRHYDSD <b>CD</b> CADFHMLSRCNSIRVEGWTWAYERPFPAGYMYILLPRGEYPEYQHWMGLNDRLS <b>C</b> RAVH
Bovine $\gamma$ B	QHT-GT
Bovine $\gamma$ D	-HAG-S
Human $\gamma$ S	LPGGQ
Bovine $\gamma$ S	LSSGGQ
C-terminal domain	
	100   120   140   160
Bovine $\gamma$ B	FRMRIYERDDFRGQWSEITDD <b>C</b> PSLQDRFHLTEVHSLNVLEGSWVLYEMPSSYRGRQYLLRPGEYRRLYLDWGAMNAKVGSLLRRVM
Bovine $\gamma$ D	HRRLIYEREDYRGQMIEITED <b>C</b> SSLQDRFHFNEIHSILNVLEGSWVLYELPNYRGRQYLLRPGEYRRLYHDWGAMNAKVGSLLRRVI
Human $\gamma$ S	YKIQIFEKGFSGQMYETTED <b>C</b> PSIMEQFHMREIHS <b>C</b> KVLEGVWIFYELPNYRGRQYLLDKKEYRKPIDWGAASPAVQSFRRIV
Bovine $\gamma$ S	YKLQIFEKGFSGQMHETTED <b>C</b> PSIMEQFHMREVHS <b>C</b> KVLEGAWIFYELPNYRGRQYLLDKKEYRKPVDWGAASPAVQSFRRIV
C-terminal extension	
	174
Bovine $\gamma$ B	DFY
Bovine $\gamma$ D	DIY
Human $\gamma$ S	E
Bovine $\gamma$ S	E

(PMSF). The suspension was sonicated then centrifuged at  $17\,000\text{ rev. min}^{-1}$  for 20 min at  $4^{\circ}\text{C}$ . The supernatant was clarified by another centrifugation at  $30\,000\text{ rev. min}^{-1}$  for 90 min at  $4^{\circ}\text{C}$  and dialysed overnight, at  $6^{\circ}\text{C}$ , against the selected buffer: 50 mM Tris-HCl, pH 7.0 (8.0 or 8.5), 1.5 mM PMSF or 150 mM phosphate (22 mM  $\text{Na}_2\text{HPO}_4$ , 28 mM  $\text{KH}_2\text{PO}_4$ , 200 mM KCl, 1.3 mM EDTA, 3 mM  $\text{NaN}_3$  and 3 mM DTT) (pH 6.8), 1.5 mM PMSF. Ethylene Imine Polymer (PEI from Hampton Research) was added to a final concentration of 0.12% and left for 10 min at room temperature before centrifugation at  $17\,000\text{ rev. min}^{-1}$  for 10 min at  $6^{\circ}\text{C}$ . All steps were checked by SDS-PAGE electrophoresis.

## 2.2. Purification of $h\gamma\text{S}$

To purify the C-terminal domain of the recombinant  $b\gamma\text{S}$ , Basak et al. [13] have used a MonoQ ion exchange chromatography. We found, however, that gel filtration chromatography was as efficient to isolate  $h\gamma\text{S}$  (note that *E. coli* proteins with a molecular weight approx. 20 kDa are rare). So, after the last centrifugation of the protein extracts, the supernatant was filtered and applied to a Sephacryl S-200 HR column, on a FPLC system (Pharmacia), equilibrated with either 50 mM Tris-HCl at the selected pH or 150 mM phosphate (pH 6.8). The  $\gamma\text{S}$  containing fractions were collected and concentrated by ultrafiltration using an Amicon cell (Biomax-5 Millipore membranes). The purity of the recombinant protein was checked by SDS-PAGE electrophoresis and mass spectrometry.

## 2.3. The C20S $h\gamma\text{S}$

The Cys20  $\rightarrow$  Ser mutation was introduced using the QuickChange<sup>TM</sup> site — directed mutagenesis kit (Stratagene). The sense sequence of the mutation primers was CTA TGA CTG TGA TTC CGA CTG TGC AG. The mutation changes the Cys codon TGC to the Ser codon TCC and introduces a *Hinf*I site. This was used to screen the clones for the presence of the mutation. One of the mutant clones was picked and sequenced to ensure the absence of other mutations. The mu-

tated plasmid was used to transform BL21(DE3) pLysS competent cells from Stratagene. The protocol for the expression and purification of the C20S recombinant crystallins was the same as for the wild-type protein.

## 2.4. Purification of $b\gamma$ -crystallins

$b\gamma$ -crystallins were prepared following the main lines of the method described in Tardieu et al. [17]. They were extracted from the cortex of young calf lenses. The cortex was separated from the nucleus (central part of the lens) by gentle stirring of the lens in 150 mM phosphate buffer (pH 6.8) for 15 min at  $6^{\circ}\text{C}$ . The cortex mixture added with 43 mM PMSF and adjusted to  $60\text{ mg ml}^{-1}$  was then crushed with a Potter crusher. The solution was then centrifuged at  $30\,000\text{ rev. min}^{-1}$  for 60 min at  $6^{\circ}\text{C}$ . The protein concentration,  $c_p$  ( $\text{g ml}^{-1}$ ), was measured with an Abbe refractometer using  $n = 1.3342 + 0.184 c_p$  and adjusted to  $50\text{ mg ml}^{-1}$ .  $\gamma$ -Crystallins were prepared from the clear supernatant fraction by gel filtration, using a FPLC system and a Superdex S-200PG column eluted with the phosphate buffer at a flow rate of  $3\text{ ml min}^{-1}$ . The  $\gamma$ -crystallin fractions were concentrated by ultrafiltration (Amicon cell with Biomax-5 Millipore membranes).

The various  $\gamma$ -crystallins were then purified by cation exchange chromatography on a MonoS HR 10/10 column. To exchange the phosphate buffer against the buffer used with the MonoS column, the total  $\gamma$  fractions were applied to a Fast Desalting column eluted with 50 mM MES (pH 6.1) (buffer A) at a flow rate of  $8\text{ ml min}^{-1}$ . The MonoS column was equilibrated with buffer A and then eluted at a flow rate of  $4\text{ ml min}^{-1}$ . A gradient from 0 to 10% buffer B (buffer A + 1 M NaCl) was applied.  $\gamma$ -Crystallin concentrations were measured by UV absorption at 280 nm using an extinction coefficient of  $1.85\text{ cm}^2\text{ mg}^{-1}$  for  $\gamma\text{S}$  and  $2\text{ cm}^2\text{ mg}^{-1}$  for the other  $\gamma$ -crystallins.

## 2.5. Electrospray mass spectrometry

The mass spectrometry measurements were made using an atmospheric pressure ionisation, single quadrupole, electrospray ionisation mass

spectrometer (ESI-MS) from Micromass. The continuous phase was 50% CH<sub>3</sub>CN/H<sub>2</sub>O run at 10  $\mu\text{l min}^{-1}$  and samples were dissolved in the continuous phase containing 0.5% v/v HCOOH. Samples which have been run on a reversed phase column were in an elution buffer mixture of CH<sub>3</sub>CN/H<sub>2</sub>O containing 0.1% v/v TFA and these samples were applied directly to the mass spectrometer. Data were collected in a series of 10-s scans over an  $m/z$  range of 750–1150 for a period of 2 min. The raw data were processed using the MassLynx 3.0 software from Micromass.

## 2.6. Determination of oligomeric states

Protein size, i.e. oligomerisation, was measured by gel filtration on a FPLC system. On a Superdex S-75 HR 10/30 column, 50  $\mu\text{l}$  of protein solutions at 20–25  $\text{mg ml}^{-1}$  were applied and eluted at 1  $\text{ml min}^{-1}$  with different buffers.

## 2.7. Small angle X-ray scattering (SAXS)

The intensity scattered by one particle as a function of the scattering vector  $s$  (where  $s = 2\lambda^{-1}\sin\theta$  and  $2\theta$  is the scattering angle), usually called the particle form factor, is the Fourier transform of the spherically averaged auto-correlation function of the electron density contrast associated with the particle [18]. When the solution is ideal, i.e. in the absence of interactions, the total scattering,  $I(0,s)$ , is the sum of the scattering of the individual particles. With solutions of monodisperse spherical particles, and in the presence of interactions, departure from ideality may simply be accounted for by a multiplying factor or interference term,  $S(c,s)$ , which is a function of the scattering angle:

$$I(c,s) = I(c,0) \cdot S(c,s)$$

$S(c,s)$  is usually called the solution structure factor. With repulsive interactions, the particles are evenly distributed and  $S(c,0)$  is lower than 1. With attractive interactions, fluctuations in the particle distribution are observed which lead to a  $S(c,0)$  value larger than 1.

The experiments were carried out using the

small angle instrument D24 using the synchrotron radiation emitted by the storage ring DCI at the Laboratory for Synchrotron Radiation, L.U.R.E. (Orsay). Data were collected using a linear position-sensitive detector with a delay line readout. The sample-to-detector distance was 1.6 m, yielding an  $s$ -increment per channel of  $0.0002454 \text{ \AA}^{-1}$  and the average recorded  $s$  range was  $0.2 \times 10^{-2} < s < 4 \times 10^{-2} \text{ \AA}^{-1}$ . The wavelength of the X-rays was  $1.488 \text{ \AA}$  (K-edge of Ni). The solution experiments were performed with a specially designed quartz cell operated under vacuum [19] that could be filled and rinsed in situ. Several successive frames, from 1 to 6 according to the protein concentration, each with a duration of 300 s, were recorded for each sample and for the corresponding buffer. The curves were scaled to the transmitted intensity and averaged when no radiation damage was observed. The intensity curves,  $I(c,s)$ , were subtracted for background and, within each series, scaled on the same relative value with a normation for concentration. When the X-ray spectra were unchanged as a function of time, the six spectra were averaged and one value of  $R_g$  was deduced. Intensities at the origin and radii of gyration were obtained using Guinier plots, i.e. plots of  $\log I(c,s)$  vs.  $s^2$  [20].

## 3. Results

### 3.1.1. $\gamma$ S-crystallin three-dimensional structure in physiological conditions

Small angle X-ray Scattering was used to characterise the structures in solution of h $\gamma$ S and b $\gamma$ S and to compare them to that of b $\gamma$ B, whose three-dimensional structure is known. The experiments shown in Fig. 1 were performed in physiological-like conditions, i.e. in phosphate buffer (pH 6.8). The  $\gamma$ S radii of gyration were found to be  $19.5 \pm 0.5 \text{ \AA}$  in this buffer (Table 2), which is consistent with the presence of monomers in solution. This result is in agreement with the ultracentrifugation experiments performed on b $\gamma$ S in phosphate buffer (pH 7.0) [12]. Moreover, as can be seen on the figure, the three curves superimpose which means that the three-dimensional structure in solution is identical in all three cases.

Table 2

Averaged radius of gyration ( $\text{\AA}$ ) of  $\gamma$ -crystallins as a function of X-ray exposure time (six successive frames of 5 min each) in different buffers<sup>a</sup>

	150 mM phosphate (pH 6.8) w DTT	50 mM Tris (pH 8.0) w DTT	50 mM Tris (pH 8.0) w/o DTT
b $\gamma$ S	19.0	19.7	21.1; 24.8 <sup>b</sup>
h $\gamma$ S	19.9	20.4	21.7; 25.5 <sup>b</sup>
h $\gamma$ S C20S	19.4	20.5	21.2; 27.9 <sup>b</sup>
b $\gamma$ B	17.6 <sup>c</sup>	16.0	17.0
b $\gamma$ D	18.6 <sup>c</sup>	18.8	19.1

<sup>a</sup>Averaged  $R_g$  values are indicated when no significantly differences between the six frame spectra are observed.

<sup>b</sup> $R_g$  values in the first frame spectra (5 min exposure) and the last frame spectra (5 min after 25 min exposure) are respectively indicated.

<sup>c</sup>Results from Finet [23].

The coincidence confirms that the relative position and orientation of the N- and C-terminal domains of  $\gamma$ S-crystallins is the same as that of the other  $\gamma$ -crystallins, as postulated by Zarina et al. [12]. Indeed, since X-ray scattering curves probe the overall shape of the particles, a different domain pairing would have resulted in visible differences in the shape of the X-ray curves.

### 3.2. Oligomeric state as a function of pH

A comparative analysis of the oligomeric state of the b $\gamma$ B, b $\gamma$ S and h $\gamma$ S as a function of pH, by gel permeation chromatography, showed a specific behaviour of  $\gamma$ S (Fig. 2). Whereas b $\gamma$ B remained essentially monomeric in the pH range

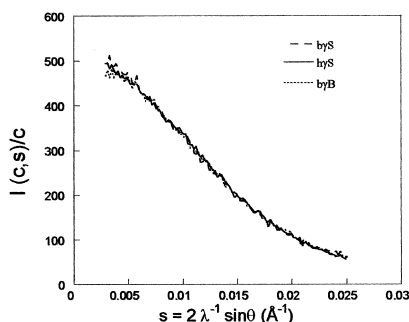


Fig. 1. SAXS patterns of b $\gamma$ S (---), h $\gamma$ S (—) and b $\gamma$ B (···) at 10 mg ml<sup>-1</sup> in phosphate buffer 150 mM (pH 6.8) at 20°C.

between 7.0 and 8.5, both  $\gamma$ S preparations yielded different species depending on the pH value. At pH 7.0, h $\gamma$ S and b $\gamma$ S preparations gave only monomers, whereas a mixture of monomers and dimers was observed at pH 8.0 as shown in Fig. 2. The same result was obtained by mass spectrometry (not shown). At pH 8.5, only h $\gamma$ S was studied; the amount of dimers was higher than at pH 8.0. The kinetics of h $\gamma$ S dimer formation was studied at pH 8.0. When the gel filtration was done immediately after the *E. coli* protein purification, only monomers were observed. The dimers began to appear after one day of storage at 6°C (Fig. 3a). The amount of dimers continued to increase during the next few days (between 3 and 5 days) and then remained identical, without any further oligomer formation, for at least 3 weeks (Fig. 4) in agreement with a monomer–dimer equilibrium. On the other hand, b $\gamma$ B and b $\gamma$ D, either prepared at pH 8.0 or pH 8.5 and then kept at 6°C in the same buffers, only yielded monomers, stable in time for at least 3 weeks, as also shown in Fig. 4.

### 3.3. A C20–C20 disulfide responsible for intermolecular dimer formation in the $\gamma$ S-crystallin

Since the cysteine  $pK$  is between pH 8.0 and 8.5, dimer formation around pH 8.0 often results

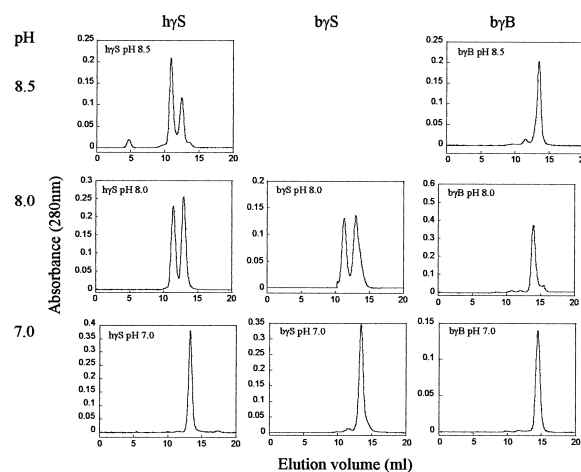


Fig. 2. pH-dependent oligomeric states of b $\gamma$ S, h $\gamma$ S and b $\gamma$ B as observed by gel filtration chromatography. All samples are in Tris buffer 50 mM either pH 8.5, 8.0 or 7.0.

from disulfides. In order to check this point, h $\gamma$ S was prepared at pH 8.0 with DTT and the protein was found only as monomers (data not shown). In addition, the dimer peak of the pH 8.0 preparation without DTT was incubated overnight with DTT. The dimers were found to be reversed to monomers (Fig. 3b).

To explain the oligomeric behaviour of the  $\gamma$ S, we looked for the residues able to form disulfides and in particular for a surface accessible cysteine that could form an intermolecular disulfide in  $\gamma$ S but not in the other  $\gamma$ -crystallins. Among the

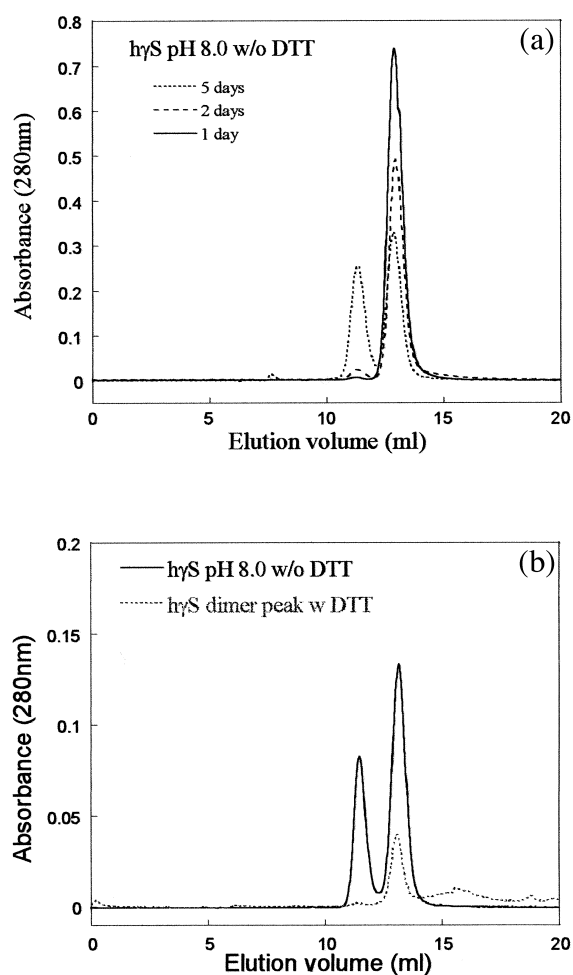


Fig. 3. (a) Kinetic of h $\gamma$ S dimer formation at pH 8.0 (Tris 50 mM without DTT) as a function of time. (b) Effect of dithiothreitol on the h $\gamma$ S dimer peak.

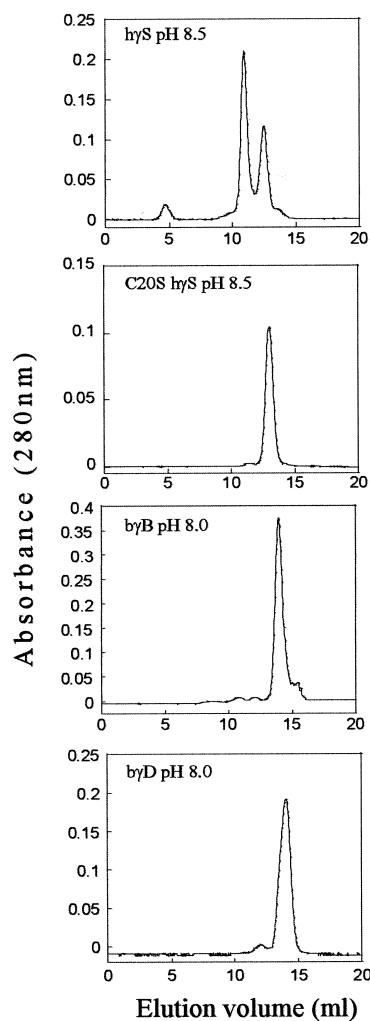


Fig. 4. From top to bottom, h $\gamma$ S\*, C20S h $\gamma$ S\*, b $\gamma$ B and b $\gamma$ D equilibration state after three weeks in Tris buffer 50 mM pH 8.0 or 8.5\* as observed by gel filtration chromatography.

$\gamma$ -crystallins that we have studied — b $\gamma$ B, b $\gamma$ D, b $\gamma$ S and h $\gamma$ S-crystallins (see Table 1) — three Cys residues are in common: Cys32, Cys78 and Cys109 (numbered 108 in  $\gamma$ D); two residues are unique to b $\gamma$ S and h $\gamma$ S: Cys20 and Cys124, and h $\gamma$ S has an additional one in position 18. Previous studies of the C-terminal b $\gamma$ S domain [13] and our results indicate that the  $\gamma$ S structure is identical to that of the other  $\gamma$ -crystallins. From the available three-dimensional structure of b $\gamma$ B [14] and from the accessibilities listed in Table 3,

only a few of these residues are partially accessible to solvent — Cys15, Cys18, Ser20 (which is Cys20 in  $\gamma$ S) and Cys22 — and could be candidates for oxidation. Cys15, only present in b $\gamma$ B, was presented as a likely candidate for intermolecular cross-linking in other studies [5], but no dimers are formed in our conditions. In the cysteine rich domain (17–22), the h $\gamma$ S contains the sequence DCDCDC — which has not been observed in any other known protein sequence — the b $\gamma$ S contains DSDCDC whereas b $\gamma$ B contains ECSSDC and b $\gamma$ D ECSSDH. In the three-dimensional structure of b $\gamma$ B [14], around 50% of Cys18 and Cys22 were found engaged in an intra-disulfide bridge. Since the originally crystallised protein did not contain any disulfide, the study indicated that oxidation may occur without unfolding. Moreover, the disulfide bridge was readily reduced in the presence of DTT. The similarity in the three-dimensional structures of the  $\gamma$ -crystallins allows the inference that the equivalent disulfide is possible between Cys18 and Cys22 of h $\gamma$ S, leaving the highly accessible Cys20 free for intermolecular disulfide formation. Consequently, we hypothesised that Cys20 was the likely candidate for the specific dimer formation in the  $\gamma$ S-crystallins and made, in this view, the h $\gamma$ S C20S mutant.

### 3.4. A h $\gamma$ S C20S mutant to check the hypothesis

If the hypothesis is correct, the h $\gamma$ S C20S mutant protein should remain monomeric at pH 8.0 or higher. The mutant was made, the protein expressed in *E. coli*, purified according to Section 2 and controlled by mass spectrometry experiments. The mutant protein prepared either at pH 8.0 or 8.5 without DTT resulted in a single peak corresponding to the monomeric species. The chromatography was repeated as a function of time. Approximately 3 weeks later, the preparation was still in a monomeric form, as shown in Fig. 4.

### 3.5. Sensitivity to oxidation of $\gamma$ S-crystallins: oligomer formation in the X-ray beam

During the course of this work, we noticed that

Table 3

Solvent accessibility of  $\gamma$ B-crystallin (PDBn4GCR) cysteines calculated as Connolly surface with Insight II<sup>a</sup>

Residue	Contact area (Å <sup>2</sup> )	Reentrant area (Å <sup>2</sup> )	Total area (Å <sup>2</sup> )
15	17.38	28.58	45.96
18	2.37	21.30	23.67
20*	20.23	20.75	40.98
22	5.12	18.13	23.25
32	0.00	0.00	0.00
41	2.61	17.07	19.68
78	0.00	0.00	0.00
109	0.09	4.87	4.96
124*	0.19	6.37	6.66

<sup>a</sup>All residues are cysteine except those with \* which are Ser20 and Lys124 in b $\gamma$ B-crystallin, but Cys20 and Cys124 in h $\gamma$ S and b $\gamma$ S-crystallin. b $\gamma$ S Cys124 was checked to be buried in the three-dimensional C-terminal domain structure (PDBn1A7H).

the samples sensitive to oxidation were even more sensitive to the oxidative conditions due to the free radicals produced by X-ray irradiation. The effect was systematically studied. For that, X-ray spectra were systematically recorded in fractionated periods of time, in order to detect any gradual change. Six spectra of 5 min each were sequentially recorded for a total exposure time of 30 min.

The samples prepared in phosphate buffer at pH 6.8, which contains DTT, did not present any clue of aggregate formation during the period of measurement, in agreement with previous work [17]. On the other hand, the series recorded with the different  $\gamma$ S at pH 8.0 without DTT, present an irreversible increase of the scattered intensity in the low angle part of the scattering curves which indicates the formation of an increasing amount of oligomeric species of increasing size (Fig. 5). The corresponding radii of gyration are shown in Table 2. The initial value of  $20 \pm 0.5$  Å for the  $\gamma$ S-crystallin is consistent with only monomers in the solution. Instead the final values of the extrapolated intensity at the origin and of the radii of gyration (approx. 28 Å) indicate that oligomers higher than dimers are formed. The addition of DTT, three hours before the measure-



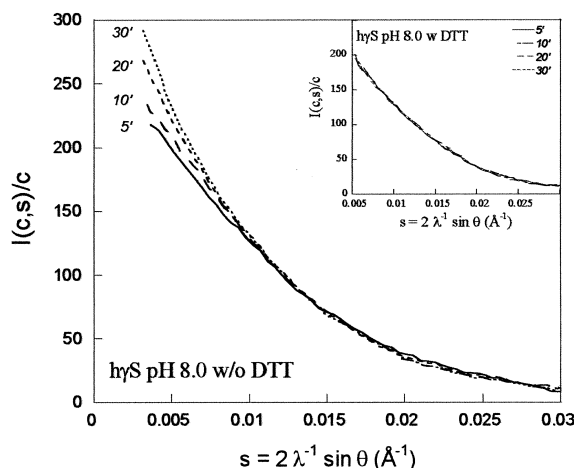


Fig. 5. h $\gamma$ S-crystallin SAXS patterns, in Tris 50 mM (pH 8.0) without DTT, as a function of X-ray exposure time (six successive frames of 5 min each). In the insert, identical sample with DTT added before X-ray experiment.

ments, was sufficient to prevent such an oligomer formation in the X-ray beam (insert in Fig. 5).

X-Ray induced oligomer formation therefore also seems to be associated to thiol oxidation. The X-ray induced oxidation, however, seems much more drastic than the oxidation occurring in storage conditions, since high MW oligomers are formed in 30 min. Moreover, h $\gamma$ S C20S oligomers were also observed in 30 min. It thus appears that new residues, probably Cys or Met, become accessible to oxidation, indicating partial unfolding in these more drastic oxidation conditions.

### 3.6. The reason why $\gamma$ S-crystallins do not opacify at low temperature

It is known for a long time that b $\gamma$ S does not display the cold cataract phenomenon. The cold cataract is a phase separation induced by decreasing the temperature. It is the consequence of the short-range attractive interactions between  $\gamma$ -crystallins at physiological pH [21,22]. X-Rays can be used to analyse the overall nature, attractive or repulsive, of the interactions in solution. Intensity curves recorded as a function of pH and protein concentration with total bovine  $\gamma$ -crystal-

lin extracts are shown in Fig. 6a. As can be seen on the figure, the intensity at low angles increases with increasing protein concentration at pH 6.8, indicating attractive interactions, and decreases at pH 4.5 when the interactions are repulsive. A similar X-ray study recently performed with purified species, b $\gamma$ B, b $\gamma$ D, b $\gamma$ E [23] indicated also that the interactions are attractive at physiological pH and still attractive at pH 8.0 (note that in some cases, it may be difficult to distinguish the attractive interactions responsible for phase separation from oligomer formation leading to precipitates. In the present study the distinction was easy to do since the oligomer formation was irreversibly increasing with time).

A comparative analysis of the interactions in solution of b $\gamma$ S, h $\gamma$ S and h $\gamma$ S C20S was done at pH 6.8 and pH 8.0. All the samples were freshly prepared in order to only have monomers in solution and only 5-min spectra were recorded to avoid possible X-ray damage. As shown in Fig. 6b, the h $\gamma$ S-crystallin curves recorded in physiological-like buffer (phosphate buffer pH 6.8) as a function of protein concentration are superimposed, which means that h $\gamma$ S do not display any significant interaction, neither attractive nor repulsive. The same result was obtained in 50 mM Tris buffer pH 8.0 as well as with the b $\gamma$ S and h $\gamma$ S C20S samples in both buffers (data not shown).

## 4. Discussion

### 4.1. Three-dimensional structure and oligomerisation

We have shown that the  $\gamma$ S structure in solution was similar to that of the other  $\gamma$ -crystallins, thus confirming the model built by Zarina et al. [12], and we have demonstrated that limited  $\gamma$ S oxidation leads to the formation of dimers. This dimer formation does not seem to be accompanied by any other conformational modification. This point is important. It is supported by the observations: (1) that the dimer is reversible, almost totally, either by adding some reducing agents or by decreasing the pH; (2) that the equilibrium ratio of the species (dimers/mono-

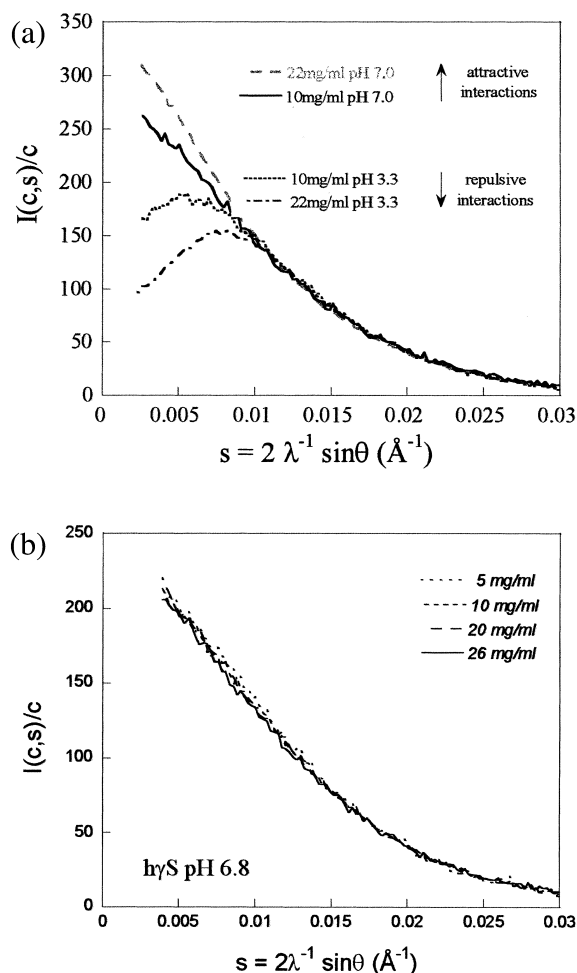


Fig. 6. (a) SAXS patterns of total b $\gamma$ -crystallins from lens nuclei, in phosphate 10 mM at pH 7.0 (attractive interactions) and pH 3.3 (repulsive interactions) at two protein concentrations [30]; (b) h $\gamma$ S-crystallins SAXS patterns in phosphate buffer 150 mM (pH 6.8) as a function of protein concentration.

mers) is maintained as a function of time and that no higher molecular weight species is formed. The involvement of Cys20, that is exposed to the solvent, in intermolecular disulfide bridge formation, was likely. It has been confirmed by the results obtained with the h $\gamma$ S C20S mutant that does not form dimers in our gentle oxidative conditions.

A study of Pande et al. [5] describes the formation of b $\gamma$ B-crystallin dimers as a function of

time, at least in part through direct disulfide bonds, whereas in the present study we only observed b $\gamma$ B monomers. Since Cys20 is not present in b $\gamma$ B, other residues have to be involved, possibly Cys15, which is absent in h $\gamma$ S. The absence of b $\gamma$ B dimers in our conditions might be due to differences in storage conditions — 6°C in our case vs. room temperature — and seems to indicate that the dimer formation of b $\gamma$ B, after long storage at room temperature without reducing agent [5], could also be accompanied by the beginning of an unfolding process.

The results obtained here confirm that the various  $\gamma$ -crystallins species may respond rather differently to an oxidative stress and that the extent of the oxidative stress may lead to different consequences. Oxidation limited to one amino acid located at the surface, leading to reversible dimers via disulfides like for h $\gamma$ S, without three-dimensional structural changes, would not be dangerous for the lens; it could even play a protective role (in acting as an oxidation ‘buffer’). The opportunity to make an internal disulfide in b $\gamma$ B and h $\gamma$ S, could also be a stabilising factor. Such a limited oxidation could, however, become dangerous if, as demonstrated by the recent study of the h $\gamma$ D R14C mutant [9], a second reactive site is present at the surface, allowing the formation of large aggregates. In this respect, it may be interesting to note that the second site that seems to be reactive in h $\gamma$ D is Cys110, which is absent in b $\gamma$ D.

On the other hand, more extensive oxidation as observed during X-ray exposure, seems to be able to reach partially buried residues and therefore to involve local denaturations. Such an oxidation could be the first step of non-specific aggregate formation possibly leading to cataract.

#### 4.2. Interactions and phase separation

The experiments presented here clarify the origin of some specific properties of  $\gamma$ S. Since the presence of a phase separation as a function of temperature is associated to the strength of the attractive interactions, the fact that the h $\gamma$ S and b $\gamma$ S solutions in physiological conditions do not display attractive interactions, like the other  $\gamma$ -

crystallin solutions [17], readily accounts for the absence of a phase separation as a function of temperature. It also explains why the presence of  $\gamma$ S in concentrated solutions of other  $\gamma$ -crystallins,  $\gamma$ B and  $\gamma$ E, may lower the phase separation temperature as reported in Liu et al. [24]. Moreover, since in the eye lens, the  $\gamma$ -crystallins that present attractive interactions are preferentially located in the centre of the lens (nucleus) whereas the  $\gamma$ -crystallins that present repulsive interactions are preferentially located at the periphery (cortex), the absence of attractive interactions is also coherent with the  $\gamma$ S location in the cortex rather than in the nucleus [25].

In previous studies of other b $\gamma$ -crystallins [5,26] the phase separation temperature was also shown to be critically dependent upon the oligomeric state. The increase in phase separation temperature could, however, rather be associated to a non-native structure of the oligomers. Indeed, we did not find such an increase of the attraction with the h $\gamma$ S mixture of monomers/dimers obtained at pH 8.0 (data not shown). The experiments presented here demonstrate instead that, with  $\gamma$ S-crystallins, the interactions in solution that control the phase separation are uncoupled from the chemical reactions that govern the formation of covalently linked oligomers.

Finally, the reason why the different  $\gamma$ -crystallins, that have the same three-dimensional structure [14,27] may have different interactions in solution and different critical temperatures, remains unclear. The point has been extensively investigated by Norledge et al. [28], the surface charge distribution has been analysed by Chirgadze and Tabolina [29], the small yet true differences in interactions between the different  $\gamma$ -crystallins have been measured recently by Finet [23], yet without providing us with any clear answer. This intriguing question therefore remains a topic to investigate in further studies.

## 5. Nomenclature

*h $\gamma$ D (or S)*: human  $\gamma$ D (or S)-crystallin

*b $\gamma$ S (B or D)*: bovine  $\gamma$ S (B or D)-crystallin

*FPLC*: fast liquid protein chromatography

*SAXS*: Small angle X-ray scattering

## Acknowledgements

The authors gratefully acknowledge the financial support of a BIOMED European contract, ‘Ageing vision’, of CNES and of the PCV program of the CNRS. F. Skouri-Panet has a post-doctoral fellowship from BIOMED. We are grateful to the members of the network for fruitful discussions and critical comments. The X-ray experiments benefited from the help of P. Vachette (LURE-ORSAY). We thank B. Frottier for the accessibility calculations.

## References

- [1] M. Delaye, A. Tardieu, Short range order of crystallin proteins account for eye lens transparency, *Nature* 302 (1983) 415–417.
- [2] S.R. Hanson, D.L. Smith, J.B. Smith, Deamidation and disulfide bonding in human lens gamma-crystallins, *Exp. Eye Res.* 67 (1998) 301–312.
- [3] Z. Ma, S.R. Hanson, K.J. Lampi, D.L.L. Smith, S.D.L. Smith, J.B. Smith, Age-related changes in human lens crystallins identified by HPLC and mass spectrometry, *Exp. Eye Res.* 67 (1998) 21–30.
- [4] A. Spector, Oxidative stress-induced cataract: mechanism of action, *FASEB J* 9 (1995) 1173–1182.
- [5] J. Pande, A. Lomakin, B. Fine, O. Ogun, I. Sokolinski, G. Benedek, Oxidation of gamma II-crystallin solutions yields dimers with a high phase separation temperature, *Proc. Natl. Acad. Sci.* 92 (1995) 1067–1071.
- [6] A. Atalay, A. Ogus, O. Bateman, C. Slingsby, Vitamin C induced oxidation of eye lens gamma crystallins, *Biochimie* 80 (1998) 283–288.
- [7] S.R. Hanson, A.A. Chen, J.B. Smith, M.F. Lou, Thiolation of the gammaB-crystallins in intact bovine lens exposed to hydrogen peroxide, *J. Biol. Chem.* 274 (1999) 4735–4742.
- [8] D.A. Stephan, E. Gillanders, D. Vanderveen et al., Progressive juvenile-onset punctuate cataracts caused by mutation of the gammaD-crystallin gene, *Proc. Natl. Acad. Sci. U.S.A.* 96 (1999) 1008–1012.
- [9] A. Pande, J. Pande, N. Asherie et al., Molecular basis of a progressive juvenile-onset hereditary cataract, *Proc. Natl. Acad. Sci. U.S.A.* 97 (2000) 1993–1998.
- [10] H.J. Aarts, N.H. Lubsen, J.G. Schoenmakers, Crystallin gene expression during rat lens development, *Eur. J. Biochem.* 183 (1989) 31–36.

- [11] C.N. Nagineni, S.P. Bhat, Lens fiber cell differentiation and expression of crystallins in co-cultures of human fetal lens epithelial cells and fibroblasts, *Exp. Eye Res.* 54 (1992) 193–200.
- [12] S. Zarina, C. Slingsby, R. Jaenicke, Z.H. Zaidi, H. Driessen, N. Srinivasan, Three-dimensional model and quaternary structure of the human eye lens protein gammaS-crystallin based on beta- and gamma-crystallin X-ray coordinates and ultracentrifugation, *Protein Sci.* 3 (1994) 1840–1846.
- [13] A.K. Basak, R.C. Kroone, N.H. Lubsen, C.E. Naylor, R. Jaenicke, C. Slingsby, The C-terminal domains of gammaS-crystallin pair about a distorted twofold axis, *Protein Eng.* 11 (1998) 337–344.
- [14] S. Najmudin, V. Nalini, H. Driessen et al., Structure of the bovine eye lens protein  $\gamma$ B ( $\gamma$ II)-crystallin at 1.47 Å, *Acta Cryst. D* 49 (1993) 223–233.
- [15] B. Bax, R. Lapatto, V. Nalini et al., X-Ray analysis of beta B2-crystallin and evolution of oligomeric lens proteins, *Nature* 347 (1990) 776–780.
- [16] M. Wenk, R. Herbst, D. Hoeger, M. Kretschmar, N.H. Lubsen, R. Jaenicke,  $\gamma$ S-crystallin of vertebrate eye lens: solution structure, stability and folding of the intact two-domain protein and its separate domains, *Biophys. Chem.* 86 (2–3) (2000) 95–108.
- [17] A. Tardieu, F. Veretout, B. Krop, C. Slingsby, Protein interactions in the calf eye lens: interactions between beta-crystallins are repulsive whereas in gamma-crystallins they are attractive, *Eur. Biophys. J.* 21 (1992) 1–12.
- [18] V. Luzzati, A. Tardieu, Recent developments in solution X-ray scattering, *Ann. Rev. Biophys. Bioeng.* 9 (1980) 1–29.
- [19] J.M. Dubuisson, T. Descamps, P. Vachette, Improved signal-to-background ratio in small angle X-ray scattering experiments with synchrotron radiation using an evacuated cell for solutions, *J. Appl. Cryst.* 30 (1997) 49–54.
- [20] A. Guinier, G. Fournet, *Small Scattering of X-rays*, Wiley, New York (1955).
- [21] A. Lomakin, N. Asherie, G. Benedek, Monte Carlo study of phase separation in aqueous protein solutions, *J. Chem. Phys.* 104 (1996) 1646–1656.
- [22] M. Malfois, F. Bonneté, L. Belloni, A. Tardieu, A model of attractive interactions to account for liquid–liquid phase separation of protein solutions, *J. Chem. Phys.* 105 (1996) 3290–3300.
- [23] S. Finet, PhD thesis, 1999.
- [24] C. Liu, N. Asherie, A. Lomakin, J. Pande, O. Ogun, G.B. Benedek, Phase separation in aqueous solutions of lens gamma-crystallins: special role of gamma S, *Proc. Natl. Acad. Sci.* 93 (1996) 377–382.
- [25] F. Veretout, M. Delaye, A. Tardieu, Molecular basis of eye lens transparency. Osmotic pressure and X-ray analysis of alpha-crystallin solutions, *J. Mol. Biol.* 205 (1989) 713–728.
- [26] N. Asherie, J. Pande, A. Lomakin et al., Oligomerization and phase separation in globular protein solutions, *Biophys. Chem.* 75 (1998) 213–227.
- [27] H.E. White, H.P. Driessen, C. Slingsby, D.S. Moss, P.F. Lindley, Packing interactions in the eye lens. Structural analysis, internal symmetry and lattice interactions of bovine gamma IVa-crystallin, *J. Mol. Biol.* 207 (1989) 217–235.
- [28] B.V. Norledge, R.E. Hay, O.A. Bateman, C. Slingsby, H.P. Driessen, Towards a molecular understanding of phase separation in the lens: a comparison of the X-ray structures of two high TC  $\gamma$ -crystallins,  $\gamma$ E and  $\gamma$ F, with two low TC  $\gamma$ -crystallins,  $\gamma$ B and  $\gamma$ D, *Exp. Eye Res.* 65 (1997) 609–630.
- [29] Y.N. Chirgadze, O.Y. Tabolina, Alternating charge clusters of side chains: new surface structural invariants observed in calf eye lens gamma-crystallins, *Protein Eng.* 9 (1996) 745–754.
- [30] F. Bonneté, M. Malfois, S. Finet, A. Tardieu, S. Lafont, S. Veessler, Different tools to study interaction potentials in  $\gamma$ -crystallin solutions: relevance to crystal growth, *Acta Cryst. D* 53 (1997) 438–447.